

Theor. Comput. Fluid Dyn. (2010) 24:111–115  
DOI 10.1007/s00162-009-0133-6

## ORIGINAL ARTICLE

Ruben Trieling · Rudi Santbergen · GertJan van Heijst ·  
Ziv Kizner

# Barotropic elliptical dipoles in a rotating fluid

Received: 15 December 2008 / Accepted: 24 June 2009 / Published online: 30 July 2009  
© The Author(s) 2009. This article is published with open access at Springerlink.com

**Abstract** Barotropic  $f$ -plane dipolar vortices were generated in a rotating fluid and a comparison was made with the so-called supersmooth  $f$ -plane solution which—in contrast to the classical Lamb–Chaplygin solution—is marked by an elliptical separatrix and a doubly continuously differentiable vorticity field. Dye-visualization and high-resolution particle-tracking techniques revealed that the observed dipole characteristics (separatrix aspect ratio, cross-sectional vorticity distribution and vorticity versus streamfunction relationship) are in close agreement with those of the supersmooth  $f$ -plane solution for the entire lifespan of the dipolar vortex.

**Keywords** Supersmooth dipole · Separatrix · Rotating fluid ·  $f$ -Plane · Laboratory experiments

**PACS** 47.32.C-, 47.32.Ef

## 1 Introduction

Dipolar vortices play an important part in large-, meso- and small-scale geophysical flows due to their self-propelling motion and robustness. The long lifespan and stability of these coherent structures have motivated researchers to look for explicit stationary solutions relevant to ideal fluid. In a comoving frame of reference, these solutions are characterized by the existence of a closed streamline (separatrix) that demarcates the interior region, where the streamlines are closed, from the exterior region, where the streamlines are open. One of the most popular dipole solutions is the Lamb–Chaplygin dipole [1,2] which is marked by a circular separatrix. This solution was suggested about a century ago and has been widely used in various studies. Dipolar vortices in geophysical flows, however, are often slightly compressed in the direction of translation which has been confirmed by laboratory experiments [3,4] and numerical simulations [5,6]. For that reason, in more recent theoretical studies [7,8], the concept of Lamb and Chaplygin was generalized for barotropic  $f$ - and  $\beta$ -plane dipoles with elliptical separatrices. Among the possible solutions there exist the so-called supersmooth solutions whose first and second vorticity derivatives are continuous at the separatrix. Such solutions are characterized by a specific separatrix aspect ratio. Because of the uniqueness of the supersmooth solution and its remarkable stability, the present research aims at finding such structures in the laboratory. Although a  $\beta$ -plane can be easily established in the laboratory, we restrict ourselves to the  $f$ -plane for which only a single (to within scaling) supersmooth solution exists.

---

Communicated by H. Aref

---

R. Trieling (✉) · R. Santbergen · G. J. van Heijst  
Fluid Dynamics Laboratory, Eindhoven University of Technology, PO Box 513, 5600 MB Eindhoven, The Netherlands  
E-mail: R.R.Trieling@tue.nl

Z. Kizner  
Departments of Mathematics and Physics, Bar-Ilan University, 52900 Ramat-Gan, Israel  
E-mail: Ziv.Kizner@gmail.com

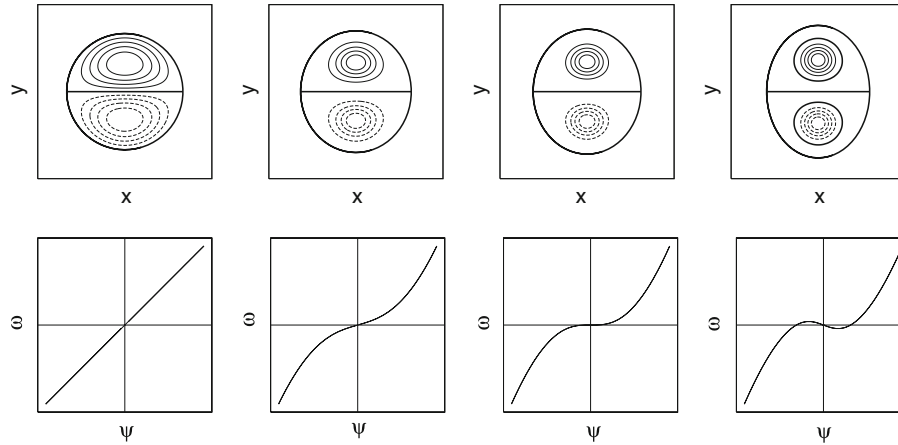


**Fig. 1** Family of elliptical barotropic  $f$ -plane dipoles with separatrix aspect ratios  $\varepsilon = 1$  (Lamb–Chaplygin solution),  $\varepsilon = 1.10$ ,  $\varepsilon = 1.16$  (supersmooth  $f$ -plane solution) and  $\varepsilon = 1.30$  (after [7]). *Upper panels*, vorticity fields. *Lower panels*, vorticity versus (comoving) streamfunction relationships in the vortex interior. The contours are plotted with a 20% interval of the maximum vorticity. *Thin solid and dashed contours* correspond to positive and negative isolines of vorticity, respectively. The *thick solid lines* indicate the zero isolines of vorticity (outside the separatrix, the vorticity is identically zero)

## 2 Theory

Elliptical barotropic  $f$ -plane dipoles, when properly scaled, represent a one-parameter family of solutions which can be parametrized by the ellipse aspect ratio  $\varepsilon = r_y/r_x$ . Here,  $r_x$  and  $r_y$  are the ellipse radii in the  $x$ - and  $y$ -axes, respectively, where the assumption is made that the dipole translates in the  $x$ -direction. Figure 1 shows four different solutions corresponding to  $\varepsilon = 1$ ,  $\varepsilon = 1.1$ ,  $\varepsilon = 1.162$  and  $\varepsilon = 1.30$ . The vorticity fields are displayed in the upper panels, whereas the vorticity versus (comoving) streamfunction relationships are shown in the lower panels. The Lamb–Chaplygin dipole is recovered as a special case, with  $\varepsilon = 1$ , in which the separatrix is a circle that encloses a region of nonzero vorticity, with the vorticity versus streamfunction relationship being linear. The main effects of the extension of the separatrix in the  $y$ -direction (for a fixed dipole translation speed  $U$  and geometrical mean ellipse radius  $a = \sqrt{r_y r_x}$ ) are sharpening of the vorticity distribution, the corresponding growth of the peak vorticities, and the change of slope of the graph of vorticity versus streamfunction at the origin. For  $\varepsilon = 1$  the slope is positive, while for  $\varepsilon = 1.30$  the slope is negative. Since this slope is a monotonic function of  $\varepsilon$ , there exists only a unique aspect ratio,  $\varepsilon \approx 1.162$ , at which the slope is zero; this specific aspect ratio also corresponds to the only elliptic  $f$ -plane dipole solution with continuous first and second normal vorticity derivatives at the separatrix [7, 8]. For this reason, in order to highlight the higher degree of smoothness compared to other elliptical solutions, this dipole solution is referred to as the supersmooth solution whose characteristics may be close to those of the dipoles observed in the laboratory.

## 3 Method

The laboratory experiments were performed in a tank with horizontal dimensions  $1.0 \times 1.5$  m that was mounted on top of a turntable. The tank was filled with water to a depth of 20 cm and the flow was allowed to adjust to a solid-body rotation for at least half an hour. The angular velocity of the turntable was set to  $0.7 \text{ rad s}^{-1}$ . A dipolar vortex was created by dragging a vertical plate, with horizontal size  $d = 25$  cm, through the fluid in the horizontal direction while simultaneously lifting the plate in the vertical direction. After the plate was removed, a well-defined quasi-steadily translating dipolar vortex emerged within a few rotation periods. The initial flow characteristics were controlled by variation of the drag speed  $V$  and the drag distance  $s$ . To obtain a quasi-two-dimensional flow, the drag speed was chosen such that the Rossby number  $Ro = V/\Omega d$  was smaller than unity. Also the drag distance was limited since otherwise a chain of dipoles was produced, much like a Von Kármán vortex street. Dye-visualization and high-resolution particle-tracking techniques were used to obtain qualitative and quantitative information about the horizontal flow field.

## 4 Results

Figure 2 shows the time evolution of a typical dipolar vortex. The interior region of the vortex was visualized by low-concentration fluorescent dye which was originally released at the front of the plate. In addition, a line of high-concentration dye was introduced at some distance from the initial position of the plate. This line of dye eventually demarcates the interior region of the dipole and facilitates the identification of the separatrix. For several initial forcing parameters and different times, the separatrix aspect ratio  $\varepsilon = r_y/r_x$  was determined by measuring the ellipse major and minor semi-axes from dye distributions as shown in Fig. 2. In order to overcome the lack of information at the rear part of the separatrix, the dye-distribution images were reflected symmetrically about the apparent axis of symmetry  $y$ , being defined as the line passing through the local vortex cores. It is seen from Fig. 3 (left panel) that the separatrix aspect ratio fluctuates around a mean value  $\bar{\varepsilon} = 1.28 \pm 0.07$  which is higher than, but close to the value  $\varepsilon \approx 1.162$  associated with the supersmooth elliptical dipole solution. The fluctuations are likely due to the inaccuracy of the measurement procedure, as well as surface waves induced by the plate.

As a second approach, the separatrix aspect ratio was determined from the streamfunction field. The latter was computed from the measured horizontal velocity field and corrected for the instantaneous translation speed of the dipole. The dipole translation speed was obtained from the observed displacements of the local vortex cores. In order to estimate the separatrix aspect ratio, the separatrix was least-square fitted with an elliptic contour. Figure 3 (right panel) shows the time evolution of the separatrix aspect ratio for two experimental dipoles as obtained from the comoving streamfunction, with the mean value being  $\bar{\varepsilon} = 1.26 \pm 0.08$ , which is close to that obtained for the dye-visualization experiments.

The measured horizontal velocity field also allows for the computation of the vorticity and the streamfunction distribution. Both quantities are plotted in Fig. 4 for a dipolar vortex with the separatrix aspect ratio  $\varepsilon = 1.18$ . Also shown, in the same figure, is the elliptic contour that was least-square fitted to the dipole separar-

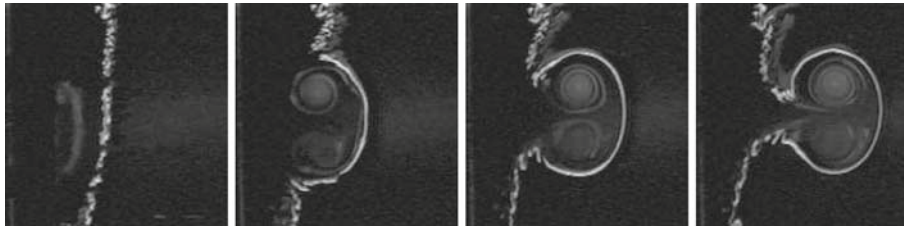


**Fig. 2** Dye visualization of a dipole propagating through a line of dye. The dye eventually demarcates the interior region of the dipole providing an indication of the separatrix aspect ratio

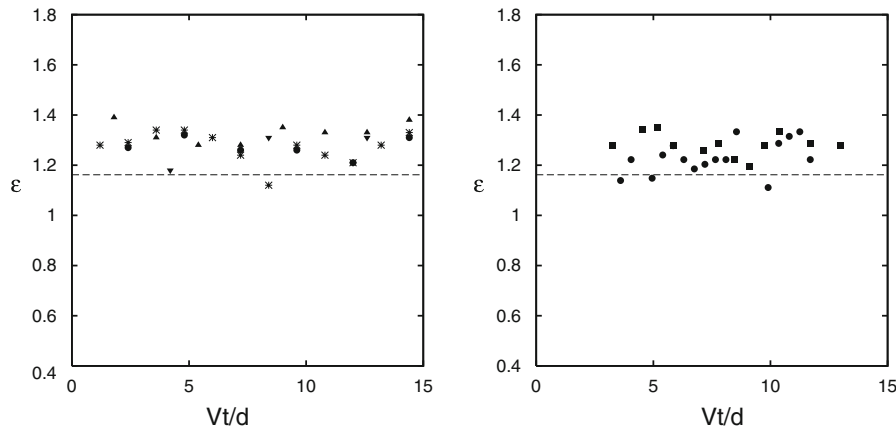


**Fig. 3** Time evolution of the separatrix aspect ratio  $\varepsilon$  for different forcing parameters. *Left panel*, as obtained from dye-visualization studies (as shown in Fig. 2);  $V = 1.0 \text{ cm s}^{-1}$ ,  $s = 4 \text{ cm}$  (asterisks),  $V = 1.5 \text{ cm s}^{-1}$ ,  $s = 9 \text{ cm}$  (upward triangles),  $V = 2.0 \text{ cm s}^{-1}$ ,  $s = 38 \text{ cm}$  (bullets), and  $V = 3.5 \text{ cm s}^{-1}$ ,  $s = 9 \text{ cm}$  (downward triangles). *Right panel*, as obtained from the comoving streamfunction;  $V = 2.25 \text{ cm s}^{-1}$ ,  $s = 18 \text{ cm}$  (bullets),  $V = 3.25 \text{ cm s}^{-1}$ ,  $s = 18 \text{ cm}$  (squares). The typical error in the measured aspect ratio is  $\pm 0.15$  in all cases. The separatrix aspect ratio for the supersmooth  $f$ -plane dipole is indicated by the dashed line

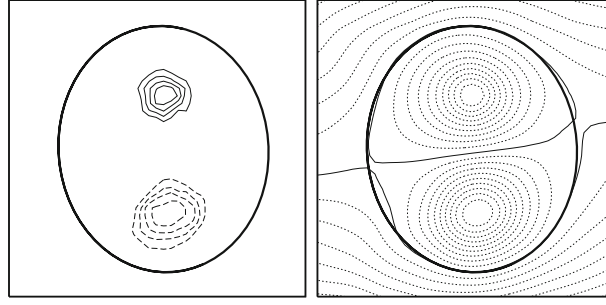


**Fig. 4** Contour plots of vorticity (*left panel*) and comoving streamfunction (*right panel*) for a dipolar vortex with separatrix aspect ratio  $\varepsilon = 1.18$ . On either side of the dipole translation axis, the contours are plotted with a 20% interval of the local extrema of vorticity and streamfunction, respectively. *Thin solid and dashed isolines* of vorticity correspond to positive and negative values of vorticity, respectively, the zero isoline being omitted. Also shown is the elliptic contour (*thick solid line*) that was least-square fitted to the separatrix whose approximate location is indicated by the *thin solid contours* (zero streamfunction isolines) in the *right panel*. Forcing parameters:  $V = 3.0 \text{ cm s}^{-1}$  and  $s = 10 \text{ cm}$

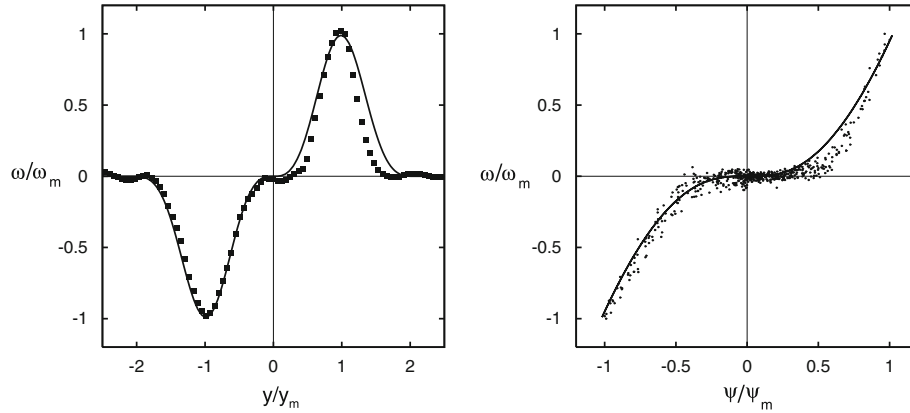


**Fig. 5** Comparison of experimental results with the supersmooth dipole solution. *Left panel*, cross-sectional vorticity distribution along a straight line passing through the dipole vorticity extrema. *Right panel*, vorticity versus comoving streamfunction relationship for the interior dipole region. The supersmooth  $f$ -plane solution is indicated by the *solid lines*. On either side of the dipole symmetry axis, both the vorticity and the streamfunction have been normalized by their local extremal values. The distance along the dipole symmetry axis  $y$  has been normalized by half the distance between the local extrema of the comoving streamfunction. Forcing parameters as in Fig. 4

atrix whose approximate location is indicated by the solid streamlines. The apparent separatrix splitting is due to the presence of a 10%–20% deviation from non-divergence in the velocity field as well as the inaccuracy in the estimated dipole translation speed. The vorticity of the dipole appears to be concentrated in two well-separated vortex cores, characteristic of sufficiently extended elliptic dipoles, and the dipole's separatrix is close to elliptic. Figure 5 (left panel) shows the corresponding cross-sectional vorticity distribution along a straight line passing through the local extrema of the comoving streamfunction. Also shown is the corresponding scatter plot of the vorticity versus comoving streamfunction for the interior dipole region (right panel). In both cases, close agreement with the supersmooth elliptical solution (solid lines) is obvious. Especially note the zero slope at which the vorticity versus streamfunction graph crosses the origin. This agreement was monitored for the entire lifespan of the dipolar vortex.

## 5 Discussion and conclusions

In the present study we have investigated the temporal evolution of concentrated barotropic  $f$ -plane dipoles whose characteristics were observed to be close to that of the supersmooth dipole solution. This agreement was obtained for the entire life span of the vortex and for a wide range of forcing parameters.

The apparent robustness of the observed dipoles seems to confirm previous numerical simulations [8] in which the ( $f$ - and  $\beta$ -plane) supersmooth dipoles were found to be the most stable among all the elliptical

dipoles in the nearly inviscid limit. In contrast, in a related numerical study on concentrated vortex dipoles [9] it was shown that various initial vorticity distributions evolve, through viscous effects, towards a specific family of dipoles parametrized by the dipole aspect ratio  $a/b$  (not to be confused with the separatrix aspect ratio), where  $a$  is the radius of the local vortex cores based on the polar momentum in half a plane (with single-signed vorticity) and  $b$  is the separation distance between the vortex core centroids. In this respect, the apparent stability of the observed dipoles in rotating-tank experiments may be merely due to the relatively large Reynolds number, which was within the range 2500–8750 based on the size and the translation speed of plate, while it was initially of the order of  $10^4$  using the ratio of single-signed circulation and kinematic viscosity.

The vorticity distribution associated with the supersmooth dipole is different, however, from the initial vorticity distributions considered in the aforementioned study involving concentrated vortex dipoles. It therefore still needs to be verified whether the supersmooth dipole should indeed evolve, through viscous effects, towards the specific family of dipoles or will it preserve its characteristics for a long time, as in the nearly inviscid limit. In this respect, it should be beard in mind that the bottom friction (Ekman layer) can have a stronger effect upon an experimental dipole than the lateral friction considered in the numerical simulations [9]. In any case, one of the effects of viscosity is smoothing of the vorticity profile in any vortical structure. Therefore, it can be expected that if viscosity makes dipoles to tend towards a specific family of shapes, this family must be supersmooth, although, not necessarily exactly elliptical.

Considering the closeness of the observed dipolar vortices to the supersmooth  $f$ -plane dipole, the latter seems to provide a better model for the observed elliptic  $f$ -plane dipoles than the Lamb–Chaplygin model.

**Acknowledgments** We thank the organizers of the IUTAM Symposium, in particular Hassan Aref and Dorte Glass for their effort and hospitality. Z.K. acknowledges the support from the Israel Science Foundation grant 628/06, and the financial support from the Netherlands Organization for Scientific Research (NWO) for his working visit at TUE. We are grateful to Enric Pallàs-Sanz for his contribution to the laboratory experiments.

**Open Access** This article is distributed under the terms of the Creative Commons Attribution Noncommercial License which permits any noncommercial use, distribution, and reproduction in any medium, provided the original author(s) and source are credited.

## References

1. Lamb, H.: Hydrodynamics, 6th edn. Cambridge University Press, Cambridge, 738 p. (1932)
2. Meleshko, V.V., van Heijst, G.J.F.: On Chaplygin's investigations of two-dimensional vortex structures in an inviscid fluid. *J. Fluid Mech.* **272**, 157–182 (1994)
3. Flór, J.B., van Heijst, G.J.F.: An experimental study of dipolar vortex structures in a stratified fluid. *J. Fluid Mech.* **279**, 101–133 (1994)
4. Velasco Fuentes, O.U., van Heijst, G.J.F.: Experimental study of dipolar vortices on a topographic beta-plane. *J. Fluid Mech.* **259**, 79–106 (1994)
5. Hesthaven, J.S., Lynov, J.P., Nielsen, A.H., Rasmussen, J.J., Schmidt, M.R., Shapiro, E.G., Turitsyn, S.K.: Dynamics of a nonlinear dipole vortex. *Phys. Fluids* **7**, 2220–2229 (1995)
6. Nielsen, A.H., Rasmussen, J.J.: Formation and temporal evolution of the Lamb dipole. *Phys. Fluids* **9**, 982–991 (1997)
7. Kizner, Z., Khvoles, R.: Two variations on the theme of Lamb–Chaplygin: supersmooth dipole and rotating multipoles. *Regul. Chaotic Dyn.* **9**, 509–518 (2004)
8. Khvoles, R., Berson, D., Kizner, Z.: The structure and evolution of elliptical barotropic modons. *J. Fluid Mech.* **530**, 1–30 (2005)
9. Sipp, D., Jacquin, L., Cosssu, C.: Self-adaptation and viscous selection in concentrated two-dimensional vortex dipoles. *Phys. Fluids* **12**, 245–248 (2000)